THE ASTROPHYSICAL JOURNAL, 463:60–68, 1996 May 20

A NEW *I*-BAND TULLY-FISHER RELATION FOR THE FORNAX CLUSTER: IMPLICATION FOR THE FORNAX DISTANCE AND LOCAL SUPERCLUSTER VELOCITY FIELD

M. BUREAU AND J. R. MOULD
Mount Stromlo and Siding Spring Observatories, Institute of Advanced Studies, The Australian National University, Private Bag, Weston Creek P.O., ACT 2611, Australia

AND

L. STAVELEY-SMITH
Australia Telescope National Facility, CSIRO, P.O. Box 76, Epping, NSW 2121, Australia
Received 1995 June 5; accepted 1995 December 4

ABSTRACT

The Fornax Cluster represents an important step in the extragalactic distance scale. Here we present a new *I*-band luminosity–H I velocity width (*I*-band Tully-Fisher) study of the cluster using an enlarged sampled of spiral galaxies in Fornax. *I*-band CCD photometry and 21 cm parameters are measured for 23 members of Fornax and compared with data for the Virgo Cluster. We obtain an accurate distance modulus of Fornax relative to Virgo of -0.06 ± 0.15 mag. The low scatter of Fornax galaxies around the Tully-Fisher relation will make the cluster an ideal calibrator once a direct measurement of its distance is obtained. Furthermore, the H I content of the galaxies does not seem affected by the cluster environment. Here we use two different absolute calibration methods which yield an absolute distance to Fornax of 15.4 ± 2.3 Mpc (absolute distance modulus of 30.94 ± 0.33 mag). A simple model yields a Local Group Virgocentric flow velocity of 224 ± 90 km s^{-1} which corresponds to a Hubble constant of $H_0 = 74 \pm 11$ km s^{-1} Mpc^{-1} from the Fornax data.

Subject headings: distance scale — galaxies: clusters: individual (Fornax) — galaxies: distances and redshifts — galaxies: photometry

1. INTRODUCTION

The Fornax Cluster is one of the most important milestones in the extragalactic distance scale: It is sufficiently *close* to the Local Group that planetary nebulae are detected in its early-type galaxies (Arnaboldi et al. 1994; McMillan, Ciardullo, & Jacoby 1993); three Type Ia supernovae have been well observed (Hamuy et al. 1991; Phillips 1993); the globular cluster system has been studied (Grillmair 1992); and surface brightness fluctuations have been measured in several early-type galaxies (Tonry 1991). Also, the cluster has been well studied using the D_n-σ and Tully-Fisher relations. With the *Hubble Space Telescope* (*HST*), we can expect more: the detection of Cepheids, Miras, and possibly the tip of the red giant branch. Fornax is sufficiently *distant* that its velocity perturbation by the Virgocentric flow is probably only of the order of 10% of its redshift.

As a cluster, Fornax is important in its own right; it has one of the highest galaxy volume densities in the Local Supercluster (Held & Mould 1994), and more than twice the central surface density of the Virgo Cluster (Ferguson & Sandage 1988). Dynamical processes in clusters have been working ad extremum in this cluster, as exemplified by the velocity dispersion and density continuity around NGC 1399 (Grillmair et al. 1994).

The Tully-Fisher relation is a property of disk galaxies which is both vitally important to the extragalactic distance scale and a key constraint in our understanding of their formation (Freeman 1979; Gunn 1988; Zwaan et al. 1995).

In this paper, we update previous studies of the Tully-Fisher relation in Fornax (Aaronson et al. 1981; Aaronson & Mould 1983; Mathewson, Ford, & Buchhorn 1992), using the improved receivers and correlators of the Parkes telescope which have become available quite recently, and increasing the number of galaxies for which optical *I*-band surface photometry is available. We describe the sample selection in § 2, the 21 cm observations in § 3, and the optical photometry in § 4. The Tully-Fisher relation is obtained and analyzed in § 5, the H I content of Fornax galaxies is studied in § 6, and § 7 discusses the consequences of our results on the Local Supercluster velocity field and on the absolute determination of distance to Fornax. We conclude briefly in § 8.

2. SAMPLE SELECTION

A sample of Fornax galaxy members suitable to use for the Tully-Fisher relation was constructed from the ESO/Uppsala Survey of the ESO (B) Atlas (Lauberts 1982) and from Ferguson (1989; *F*-numbered objects). The selection criteria were based on the dynamics of the cluster (Held & Mould 1994) and designed to include only "normal" galaxies. Galaxies were required to be located within 6° of NGC 1399, considered to be the center of the cluster, and to possess a redshift $cz \leq 2520$ km s^{-1} (when available), corresponding to a 3 σ criterion around the mean heliocentric velocity of Fornax of 1450 km s^{-1}. Only galaxies of type S0/a and later were included. Interacting or disturbed galaxies and multiple systems were rejected. An axial ratio $b/a \leq 0.721$ ($i \geq 45°$) was also required. Priority for observations was given to galaxies with a large apparent diameter. We believe our sample to be complete down to a major axis diameter of 1.'3, excluding the S0/a galaxies NGC 1380A and NGC 1386, which are not detected in H I (Schröder and Richter 1995).

3. 21 CENTIMETER OBSERVATIONS

A total of 41 galaxies from the constructed sample were observed at 21 cm. The observations were made at the 64 m Parkes telescope on three runs: 1990 January 31–February 8, 1990 April 10–16, and 1994 August 5–10. The beamwidth of the Parkes telescope is 15′ at 21 cm.

For the 1990 runs, the system temperature of the receiver was $\simeq$40 K. A 1024 channel, 1 bit autocorrelator (Ables et al. 1975) was used and configured into four quadrants of 256 channels and bandwidth 10 MHz. Two quadrants were used for each polarization, only one being used where the redshift of the source was known. Otherwise, the two quadrants were offset by 7.5 MHz, providing a 17.5 MHz overall band which was centered on Fornax mean heliocentric velocity. This yielded a velocity coverage of 2111 km s^{-1} and 3694 km s^{-1}, respectively (in the radio convention). After Hanning smoothing, the velocity resolution was 16 km s^{-1}.

For the 1994 run, an upgraded receiver was used with a system temperature of $\simeq$25 K. The new AT correlator (Wilson et al. 1992) was used with 1024 channels covering a bandwidth of 32 MHz. This yielded a velocity coverage of 6754 km s^{-1}. After Hanning smoothing, the velocity resolution was 13 km s^{-1}, slightly better than the 1990 observations. For both the 1990 and 1994 observations, beam switching between source and sky was used, with a switching rate of 5 minutes. Where possible, identical tracks in azimuth and elevation were used for source and sky.

The data from all runs were edited, spectra for each polarization were averaged and flux calibrated, and then both polarizations were added. Subsequently, a polynomial was fitted to the line-free portion of the spectrum and subtracted, and the data were Hanning smoothed. All 21 cm profile analysis was done using the Spectral Line Analysis Package (SLAP; Staveley-Smith 1985). Twelve galaxies were observed during both the 1990 and 1994 runs. The data for those galaxies were combined with a weight inversely proportional to the square of their rms noise. The data from 1990 were resampled before being combined, using the 1994 data as a template.

Twenty-three galaxies out of 41 were detected in H I. For those galaxies, total H I flux ($F_{\rm H\,I}$), velocity width at the 20% (ΔV_{20}) and 50% (ΔV_{50}) level, observed heliocentric velocity (V_{50}) in the optical convention ($c\Delta\lambda/\lambda_0$) taken as the center of the profile at the 50% level, and signal-to-noise ratio (S/N) defined as peak flux/σ_f were measured with SLAP. The results are shown in Table 1, and the Hanning-smoothed profiles are shown in Figure 1. No cosmological corrections were applied to the measured quantities. Following the work of Roth, Mould, & Staveley-Smith (1994), who studied random and systematic algorithmic errors as well as procedural errors using different line width assessing methods, it was decided to use a one-sided Gaussian fit on each side of the profiles to measure line widths. The velocity and line width errors quoted here are also based on Roth et al., taking into account the difference between our S/N definition and their ($F_{\rm H\,I}/\Delta V_{20}\sigma_f$). For the 18 galaxies which were not detected in H I, the expected optical velocity (v_0) (where available) and the profile noise (σ_f) are presented in Table 2. Both tables indicate on which run the observations were made, or if they are combined data.

A few spectra show peculiar features. The spectrum for IC 1913 (357-G16) shows a narrow peak (width 69 km s^{-1}) at a velocity 305 km s^{-1} higher than the peak corresponding to the galaxy. The spectrum for NGC 1437B (358-G61) also has a second peak (width 132 km s^{-1}), this time at a velocity 604 km s^{-1} lower than the expected one. F35 shows a complex spectrum with three peaks at velocities of 1274, 1658, and 1803 km s^{-1} (Fig. 1). The nature of this spectrum is not understood, and no optical velocity was available for F35; follow-up observations for this object would be inter-

TABLE 1

OPTICAL AND 21 CENTIMETER PARAMETERS

Galaxy (1)	F_{HI} (Jy km s^{-1}) (2)	ΔV_{20} (km s^{-1}) (3)	ΔV_{50} (km s^{-1}) (4)	$\log(\Delta V^i_{20})$ (km s^{-1}) (5)	v_0 (km s^{-1}) (6)	i (deg) (7)	I_{tot} (mag) (8)	I^c_{tot} (mag) (9)	21 cm Obs (10)
357-G7	13.4 ± 2.7	153.2 ± 4.5	95.2 ± 6.5	2.190 ± 0.013	1121.2 ± 3.3	82 ± 3	13.28 ± 0.10	12.97 ± 0.18	Feb 90
357-G12	23.3 ± 3.5	146.3 ± 4.5	131.0 ± 6.5	2.269 ± 0.056	1568.6 ± 3.3	52 ± 9	12.46 ± 0.11	12.35 ± 0.15	Feb 90
357-G16 (IC 1913)[a]	6.3 ± 1.3	197.4 ± 4.5	157.1 ± 6.5	2.298 ± 0.010	1451.0 ± 3.3	84 ± 3	13.17 ± 0.03	12.65 ± 0.11	Combi
357-G25	1.5 ± 0.6	196.2 ± 70.4	140.4 ± 57.0	2.326 ± 0.156	1737.2 ± 33.0	68 ± 1	13.70 ± 0.03	13.41 ± 0.07	Aug 94
357-G26 (NGC 1326)	26.5 ± 2.7	256.4 ± 3.2	240.1 ± 2.8	2.559 ± 0.037	1360.1 ± 1.4	45 ± 5	9.47 ± 0.02	9.36 ± 0.06	Aug 94
F35[b]	...	...	...	...	...	61 ± 2	14.46 ± 0.07	14.29 ± 0.10	Aug 94
358-G9 (NGC 1351A)	7.9 ± 2.4	246.2 ± 4.5	209.9 ± 6.5	2.391 ± 0.008	1360.1 ± 3.3	90 ± 0	12.37 ± 0.02	11.71 ± 0.13	Feb 90
358-G13 (NGC 1350)	18.1 ± 3.6	408.8 ± 4.5	390.3 ± 6.5	2.658 ± 0.014	1905.0 ± 3.3	64 ± 4	9.07 ± 0.02	8.81 ± 0.06	Feb 90
418-G8[a]	9.2 ± 1.4	155.6 ± 4.5	134.2 ± 6.5	2.350 ± 0.027	1192.7 ± 3.3	44 ± 3	12.80 ± 0.03	12.71 ± 0.06	Feb 90
358-G15	1.5 ± 0.2	95.2 ± 4.5	77.4 ± 6.5	2.101 ± 0.032	1388.4 ± 3.3	49 ± 4	13.87 ± 0.04	13.76 ± 0.07	Combi
358-G16[c]	1.2 ± 0.5	75.4 ± 13.9	30.6 ± 22.6	...	1697.6 ± 11.3	...	...	...	Combi
358-G17 (NGC 1365)	150.8 ± 7.5	406.6 ± 1.0	371.2 ± 1.5	2.760 ± 0.036	1635.9 ± 0.8	44 ± 5	8.31 ± 0.05	8.17 ± 0.12	Combi
418-G15 (NGC 1406)	34.0 ± 5.1	353.0 ± 4.5	308.9 ± 6.5	2.548 ± 0.006	1074.8 ± 3.3	90 ± 0	10.65 ± 0.01	9.97 ± 0.13	Feb 90
358-G49 (NGC 1427A)	23.1 ± 1.2	118.8 ± 1.0	83.4 ± 1.5	2.204 ± 0.037	2027.8 ± 0.8	48 ± 5	12.26 ± 0.04	12.14 ± 0.09	Aug 94
358-G51	3.2 ± 1.0	150.4 ± 13.9	112.3 ± 22.6	2.231 ± 0.040	1734.0 ± 11.3	62 ± 1	12.54 ± 0.03	12.28 ± 0.06	Feb 90
419-G4 (NGC 1425)	56.4 ± 5.6	378.6 ± 4.5	355.5 ± 6.5	2.617 ± 0.006	1512.6 ± 3.3	66 ± 1	9.82 ± 0.04	9.50 ± 0.07	Aug 94
358-G60	12.3 ± 1.2	94.6 ± 1.0	68.8 ± 1.5	1.983 ± 0.005	803.3 ± 0.8	80 ± 2	15.10 ± 0.06	14.77 ± 0.15	Aug 94
358-G61 (NGC 1437B)	3.4 ± 0.5	143.3 ± 4.5	98.4 ± 6.5	2.176 ± 0.014	1497.4 ± 3.3	73 ± 0	12.17 ± 0.03	11.90 ± 0.11	Aug 94
358-G63	27.5 ± 5.5	320.8 ± 4.5	287.8 ± 6.5	2.509 ± 0.006	1932.4 ± 3.3	84 ± 2	10.71 ± 0.02	10.34 ± 0.15	Feb 90
302-G9[a]	16.1 ± 5.6	181.0 ± 4.5	137.8 ± 6.5	2.259 ± 0.011	987.3 ± 3.3	85 ± 3	13.23 ± 0.03	12.88 ± 0.16	Feb 90
359-G3[a]	6.7 ± 1.7	159.1 ± 4.5	113.0 ± 6.5	2.241 ± 0.016	1574.2 ± 3.3	66 ± 3	12.73 ± 0.03	12.43 ± 0.07	Feb 90
359-G6 (NGC 1484)[a]	12.0 ± 2.4	195.9 ± 4.5	132.3 ± 6.5	2.299 ± 0.011	1019.5 ± 3.3	80 ± 3	12.24 ± 0.03	11.79 ± 0.10	Feb 90
359-G16	5.1 ± 1.8	139.0 ± 4.5	115.7 ± 6.5	2.186 ± 0.015	1405.6 ± 3.3	65 ± 1	14.32 ± 0.06	14.08 ± 0.10	Combi

[a] Optical parameters are from Mathewson et al. 1992.
[b] Object detected in H I, but parameters could not be measured due to the peculiar nature of the spectra.
[c] No optical parameters available either from this paper or from Mathewson et al. 1992.

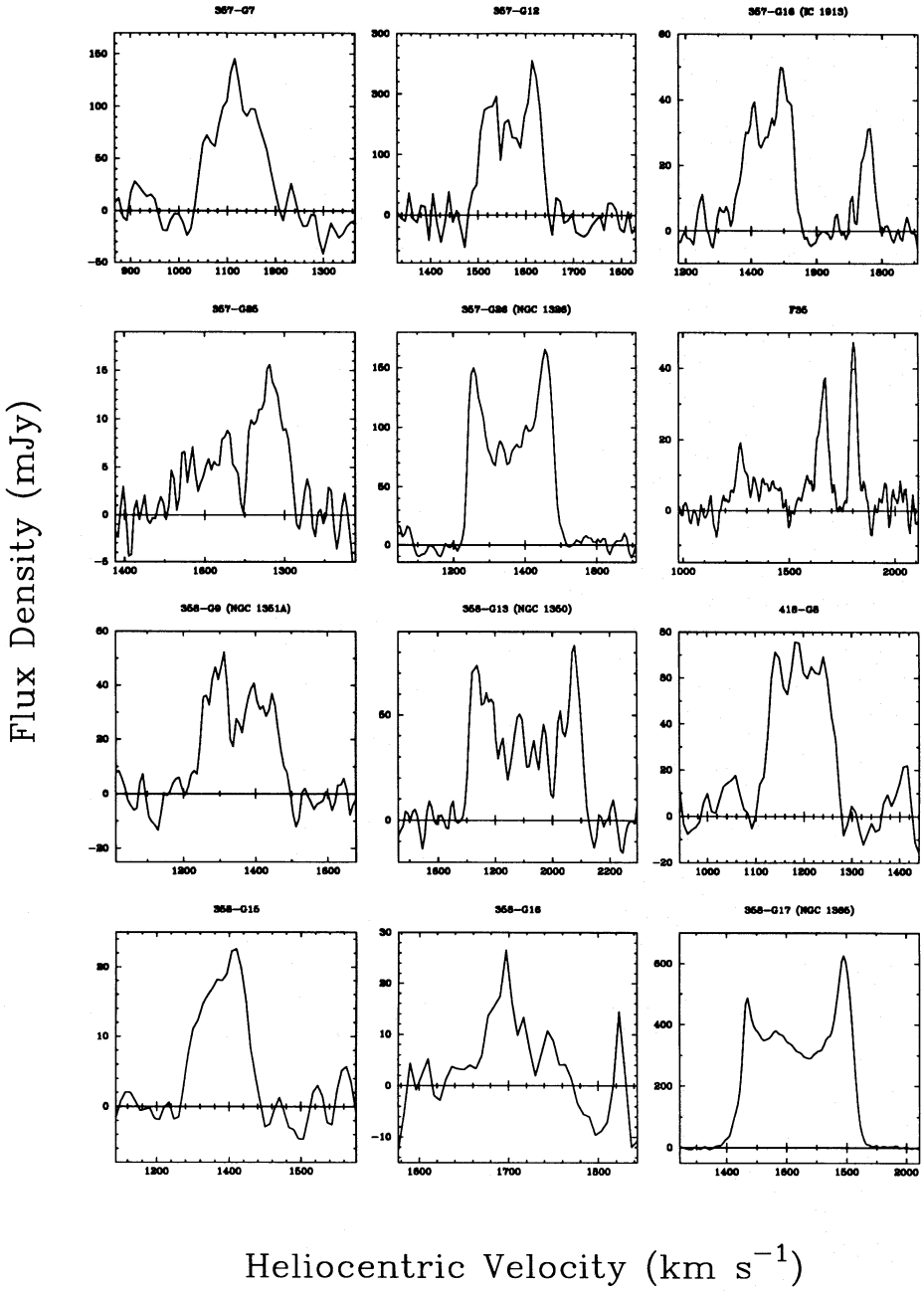

FIG. 1.—21 cm line profiles of detected galaxies. Velocities are heliocentric.

esting. It should be noted, however, that observations for NGC 1316C (357-G27) and F35 were carried out at offset positions to avoid confusion between the two sources.

4. OPTICAL PHOTOMETRY

I- and *V*-band photometry of the sample galaxies was done at the f/8 focus of the 1 m telescope at Siding Spring Observatory on two runs: 1994 October 10–12 and 1994 December 6–12. A 2250 × 1152 GEC CCD was used on both runs, with a scale of 0.″6 pixel^{-1}. Exposure times varied typically between 10–15 minutes in *I* and 5–10 minutes in *V* except for very bright objects. Graham's (1982) *E*-region standards and Landolt's (1992) standards corrected to the Cousins (SAAO) system (Bessell 1995) were observed at regular intervals during the night. All observations reported were done under photometric conditions.

The images were bias-subtracted and flat-fielded using standard techniques in IRAF. Photometric correction equations including a color-correction term $(V-I)$ were derived from the photometry of the standards. Aperture correction was used when necessary. Han's (1991) SFOTO package was used for most of the remaining data processing. After masking foreground stars, elliptical isophotes were fitted to the galaxies using GASP. Those stars were then interpolated over, and the surface brightness profile and growth curve (integrated magnitude vs. surface brightness) was obtained. Because of the high surface brightness of the sky in the *I* band and the small slope of the growth curve in the outer region of galaxies, an integrated *I* magnitude up to the last reliable measurement of surface brightness was measured and then extrapolated to infinity assuming an exponential disk in the outer part of the profile (Han 1991).

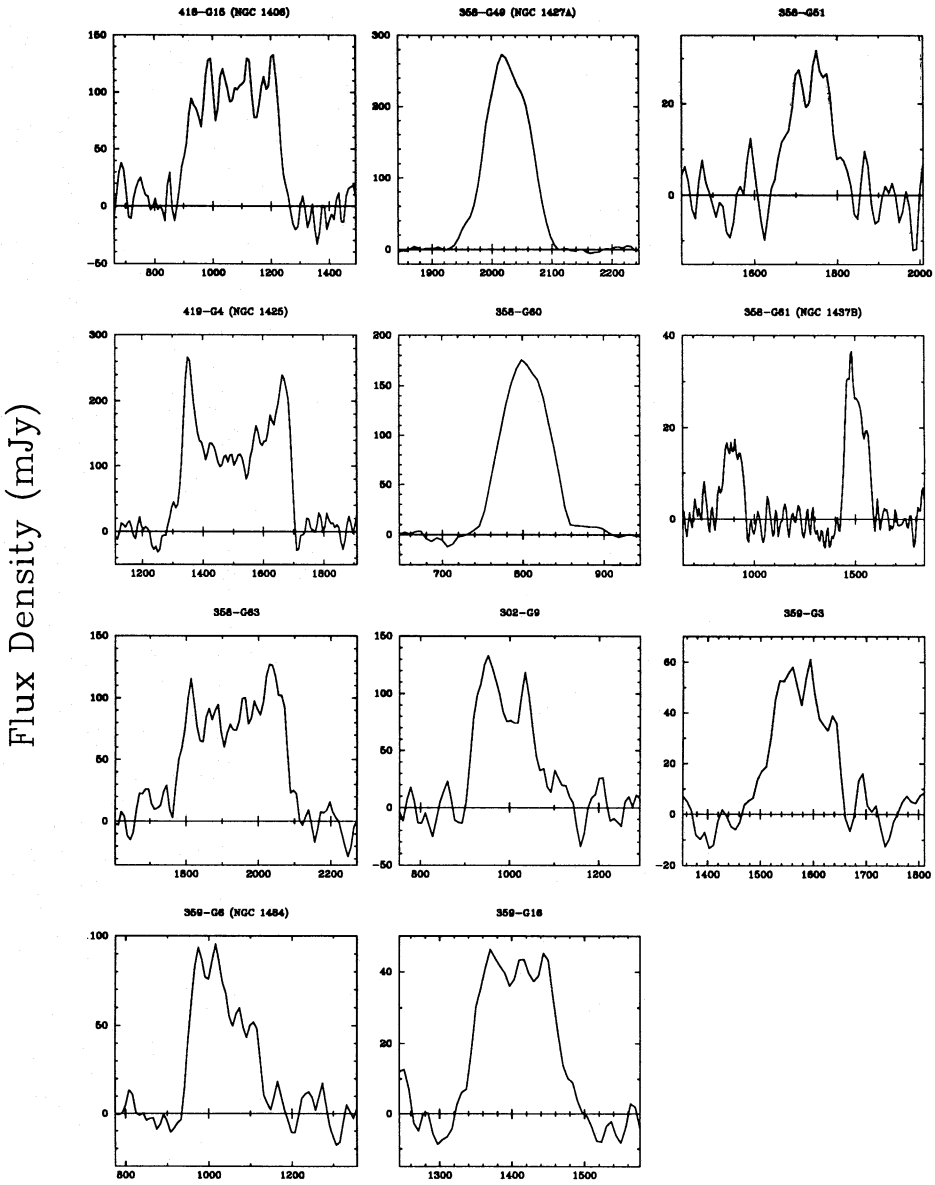

FIG. 1—*Continued*

This yields a total noncorrected integrated I magnitude (I_{tot}) for the galaxies. The inclination of the galaxies was also calculated from the fitted isophotes, assuming an intrinsic axial ratio of 0.2 for edge-on systems.

Because the limit of our sample is at a redshift of $z = 0.008$, K-correction to I_{tot} was neglected (corrections are smaller than 0.008 mag). We corrected for Galactic extinction and internal absorption in the external galaxy. The Galactic extinction was taken to be 44% of that in B as given in The Surface Photometry Catalogue of the ESO/Uppsala Galaxies (Lauberts & Valentijn 1989) from the work of Burstein & Heiles (1982). The internal absorption was taken from Han (1991) and is a function of galaxy type and inclination. A total corrected integrated I magnitude was thus obtained (I^c_{tot}).

Out of the 23 galaxies detected in H I, 10 were observed on the October run and eight were observed on the December run; 358-G60 was observed on both runs because of its faintness. Of the remaining six galaxies, five have photometric data available from Mathewson et al. (1992). In order to use their photometry to complement our data, we compared their total *uncorrected* I magnitude with ours for six galaxies which overlap their sample and for which we have photometry. The difference between our values and theirs was found to be -0.04 ± 0.14, and so their results will be used directly for the five relevant galaxies. The corrections mentioned previously have been applied to the *uncorrected* photometry results. The photometric data for the 22 galaxies analysed are shown together with the H I data in Table 1. One galaxy, 358-G16, remains with H I but no optical data, and so it will not be used for the Tully-Fisher analysis. Because of the peculiar nature of the F35

TABLE 2

21 cm NON-DETECTIONS

Galaxy	v (km s^{-1})	σ_f (mJy)	Observing Date
357-G14 (IC 1909)	...	6.02	1994 Aug
F18	...	4.37	1994 Aug
357-G27 (NGC 1316C)	1956	42[a]	1994 Aug
358-G10	1703	8.34	1990 Feb
F91	...	4.32	1994 Aug
F95	1403	6.33	1994 Aug
358-G19	1254	4.16	1994 Aug
358-G21 (NGC 1373)	1376	4.77	1994 Aug
358-G26 (IC 1963)	1639	5.02	Combined data
358-G29 (NGC 1381)	1793	3.20	1994 Aug
358-G42	1042	4.34	Combined data
358-G43	1372	4.00	Combined data
358-G50	1217	6.19	Combined data
358-G58 (NGC 1437)	1217	5.61	Combined data
358-G60	1856	8.76	Combined data
359-G2	1460	4.13	1994 Aug
359-G13	1408	2.96	Combined data
359-G18	...	4.78	1994 Aug

[a] Large noise due to a standing wave created between the primary focus cabin and the antenna surface.

H I spectrum, F35 will also be discarded for the Tully-Fisher analysis.

5. TULLY-FISHER RELATION

The I-band Tully-Fisher relation for the 21 galaxies for which both H I profiles and optical photometry are available is shown in Figure 2, plotting $I^c_{\rm tot}$ versus log (ΔV^i_{20}), where ΔV^i_{20} is the velocity width at the 20% level corrected for inclination (see Table 1). A linear regression weighted by the error on the magnitude was done on magnitude versus velocity width and is also shown in Figure 2. We obtained

$$I^c_{\rm tot} = (10.45 \pm 0.02) - (8.68 \pm 0.10)[\log (\Delta V^i_{20}) - 2.5] \ . \quad (1)$$

To look for differences in the intercepts of the Tully-Fisher relation between clusters, this form of regression is to be preferred over other methods in the absence of serious selection effects (Feigelson & Babu 1992).

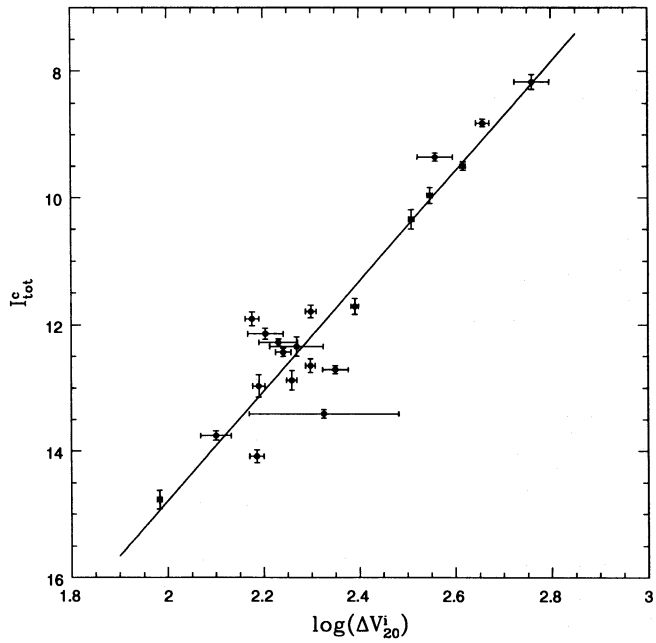

FIG. 2.—Tully-Fisher diagram for the Fornax Cluster. The line represents the weighted linear regression fit to the data.

It should be noted that the relation still holds well at the faint luminosities we reach, despite a number of factors which could affect it for such galaxies: increased support of the disk by turbulent motions and higher dark matter content in late-type spirals could change the slope in the relation or induce nonlinearity in it, while variation in the intrinsic axial ratio of the disks would increase the scatter. In addition, because our absolute "limiting" magnitude is faint, better than $M_I = -16$, assuming a distance modulus to Fornax of 30.94 (see § 7), the regression coefficients have little selection bias whatever the shape of the galaxy luminosity function (Bicknell 1992).

Mould et al. (1991) quote a Tully-Fisher relation of $I^c_{\rm tot} = (10.45 \pm 0.08) - (9.77 \pm 0.54)[\log (\Delta V^i_{20}) - 2.5]$ for their Virgo and Ursa Major calibration galaxies (assuming equal distance for both clusters), based on the average of the regression of magnitude on velocity width, and velocity width on magnitude. Taking instead a regression of magnitude on velocity width only and assuming a constant uncertainty of 0.08 mag on $I^c_{\rm tot}$ and 0.03 on log (ΔV^i_{20}) for their data, we calculated a new fit for the Virgo galaxies only. We obtained

$$I^c_{\rm tot} = (10.42 \pm 0.08) - (8.87 \pm 0.51)[\log (\Delta V^i_{20}) - 2.5] \ , \quad (2)$$

which slope agrees well, within the errors, with our Fornax fit. This result shows not only that both clusters have a similar slope, but that they lie at an almost equal distance from our Galaxy. Using equations (1) and (2), we calculated the individual distance modulus for each galaxy relative to the fit of the other cluster. This yielded a weighted mean distance modulus of Fornax relative to Virgo of 0.02 ± 0.04 mag.

Since the slopes calculated for Fornax and Virgo are very similar and the slope of the Tully-Fisher relation should be unique, we decided to merge both sets of data to obtain a common slope for both clusters. We did this by offsetting in magnitude the Fornax Cluster data (subtracting Fornax relative distance modulus to Virgo) and minimizing the "y" residuals of both clusters around a common-fitted Tully-Fisher relation, taking into account the errors on both axis. We minimized the quantity

$$\chi^2 = \sum_{\rm Fornax} \frac{[y - d - (ax + b)]^2}{(a\Delta x)^2 + \Delta y^2} + \sum_{\rm Virgo} \frac{[v - (au + b)]^2}{(a\Delta u)^2 + \Delta v^2} \ , \quad (3)$$

where $(x, y) = [\log (\Delta V^i_{20}) - 2.5, I^c_{\rm tot}]$ for Fornax data, $(u, v) = [\log (\Delta V^i_{20}) - 2.5, I^c_{\rm tot}]$ for Virgo data, and where a, b, d are the three parameters to fit; a is the slope of the Tully-Fisher relation, b is the zero point for the Virgo Cluster $\{I^c_{\rm tot} = b + a[\log (\Delta V^i_{20}) - 2.5]\}$, and d is the distance modulus of Fornax relative to Virgo. Doing this three-parameter χ^2 minimization, we obtain $a = -8.96 \pm 0.37$, $b = 10.42 \pm 0.13$ mag, and $d = -0.04 \pm 0.15$ mag. However, the χ^2 obtained this way is large. Therefore, we decided to introduce in the denominator of our χ^2 an additional constant term representing the intrinsic scatter in the Tully-Fisher relation. A value of $\Delta m = 0.40$ mag for both clusters yields a χ^2 of 41, similar to the number of degrees of freedom. This way, we obtain $a = -8.78 \pm 0.41$,

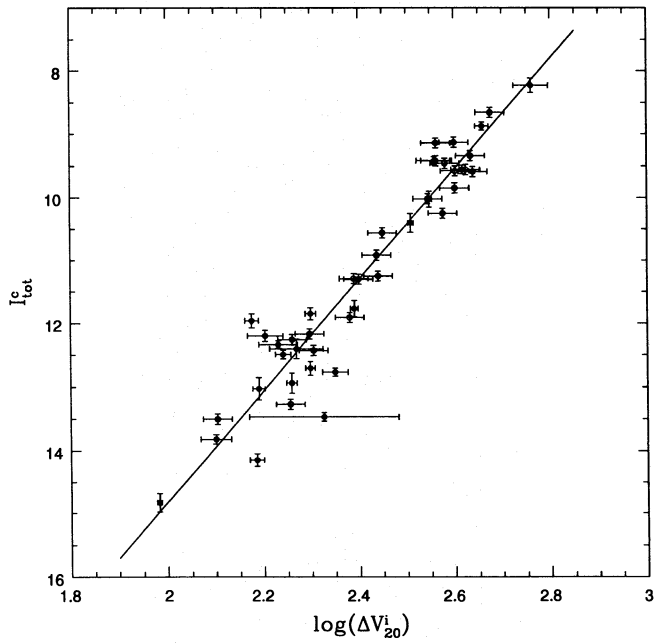

FIG. 3.—Tully-Fisher diagram for the offset Fornax data and Virgo data. The line represents the χ^2 minimization fit.

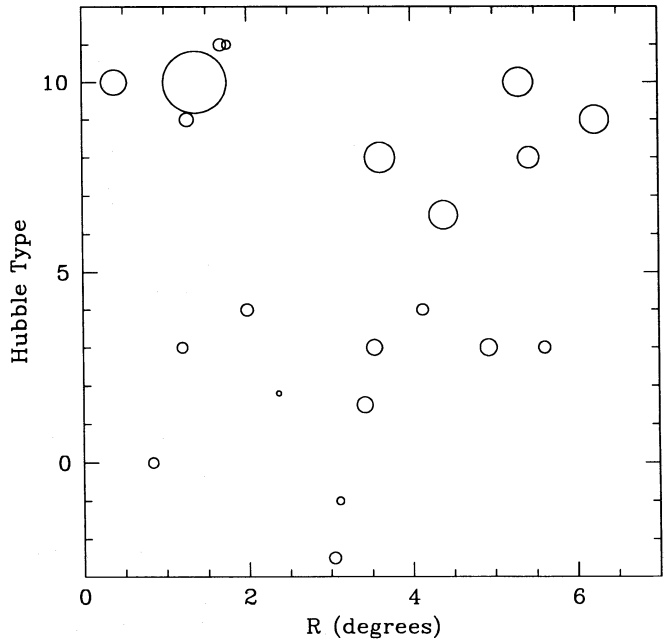

FIG. 4.—H I mass to total I-band infrared luminosity ratio ($M_{H\,I}/L_I$) of sample galaxies, as a function of projected radius from Fornax center and morphological type (type 11 corresponds here to non-Magellanic irregulars). The *area* of the circles is proportional the $M_{H\,I}/L_I$ ratio.

$b = 10.43 \pm 0.10$ mag, and $d = -0.06 \pm 0.15$ mag. Those are the adopted values. The errors are larger than those in the linear regression fit to the Fornax data because we are now taking into account the error on the velocity width and because we have to offset part of the data. The offset Fornax data, the Virgo data, and the resulting χ^2 fit are shown in Figure 3.

6. THE H I CONTENT OF FORNAX GALAXIES

The formation and evolution of spiral galaxies in a cluster environment will, at some level, be different from that in an isolated environment. Processes such as tidal stripping, ram pressure sweeping, and mergers may modify the luminous and dark mass distribution. While the light distribution is generally unaffected, it is known that spirals in the inner parts of clusters are often H I deficient compared to field spirals (e.g., in Coma: Chicarini, Giovanelli, & Haynes 1983; Bothun, Schommer, & Sullivan 1984) and that their H I disks are often truncated (e.g., in Virgo: Giovanelli & Haynes 1983, Cayatte et al. 1990). Fornax is a dense and compact cluster, so the question of whether environmental effects affect our measured H I rotational velocities arises. Various groups have compared the rotation curve of cluster and field spirals with contradictory results: Burstein et al. (1986), Rubin, Whitmore, & Ford (1988), and Whitmore, Forbes, & Rubin (1988) find that the rotation curve and mass distribution of field and cluster spirals differ (falling rotation curves and shallower M/L gradients in clusters), while Chincarini & de Souza (1985) and Guhathakurta et al. (1988, using H I deficient galaxies) find no significant differences. Furthermore, Mould et al. (1995) find that many clusters do not show H I deficiency in their galaxies.

Our data do not provide any spatial information concerning the H I distribution in the sample galaxies, so we cannot say if the shapes of the rotation curves have been affected by their environment. On the other hand, we do have information on the total H I content of the galaxies. Figure 4 shows the *distance-independent* ratio of the H I mass and the total I-band infrared-luminosity ($M_{H\,I}/L_I$) for the sample galaxies as a function of projected radius from the cluster center and morphological type. We can see the expected increase of $M_{H\,I}/L_I$ with morphological type, but no significant trend is seen with distance from the cluster center. This seems to indicate that the cluster is fairly homogeneous regarding gas content. That is, if the H I content of Fornax galaxies is different than for field galaxies, the cluster can only be affected as a whole. Figure 5 shows a comparison of the $M_{H\,I}/L_I$ ratio for Fornax and Ursa Major galaxies as a function of galaxy type. For Fornax, the data

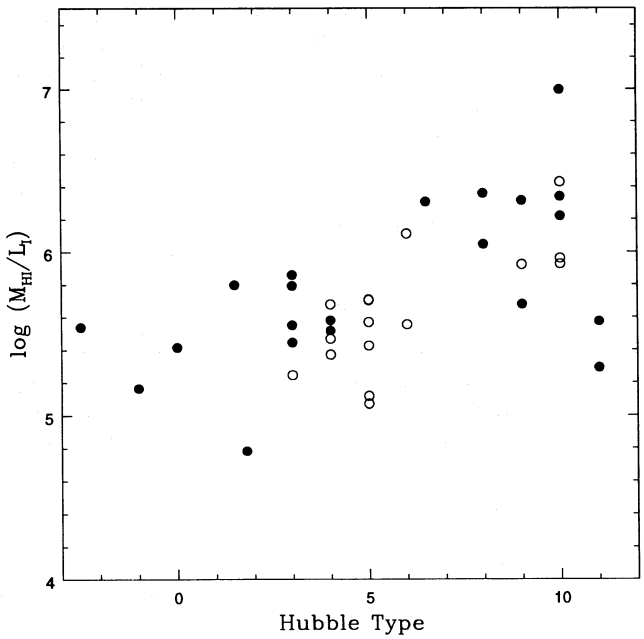

FIG. 5.—H I mass to total I-band infrared luminosity ratio ($M_{H\,I}/L_I$) of sample and Ursa Major galaxies, as a function of morphological type. Filled circles represent Fornax galaxies, and open circles represent Ursa Major galaxies.

TABLE 3

FORNAX DISTANCE MODULUS RELATIVE TO VIRGO: COMPARISON

Method	$\Delta M_{\text{Fornax}-\text{Virgo}}$ (mag)	Reference
I-band Tully-Fisher relation	-0.06 ± 0.15	1
Planetary nebulae luminosity function	0.24 ± 0.10	2
Surface brightness fluctuation	-0.16 ± 0.13	3
Globular cluster luminosity function	-0.11 ± 0.23	4
Type Ia supernovae	0.09 ± 0.14	5
Globular cluster luminosity function	-0.5 ± 0.2	6
L-Σ relation for dE	-0.16 ± 0.14	7
IR (H-band) Tully-Fisher relation	-0.25 ± 0.23	8
D_n-σ relation for E	0.14 ± 0.18	9
L-σ-Σ relation for E	-0.14 ± 0.43	10
L-Σ relation for dE	-0.02 ± 0.20	11
D_n-σ relation for E	0.21	12
L-Σ relation for dE	-0.5 ± 0.2	13
IR (H-band) Tully-Fisher relation	-0.20 ± 0.25	14
	0.03 ± 0.20	15
Revision of Visvanathan & Sandage 1977	0.16 ± 0.17	16
Color-magnitude relation for S0 and E	0.32 ± 0.23	17
Globular cluster magnitude	0.70 ± 0.15	18
Magnitude of brightest galaxies	0.4	19
Magnitude and diameter of brightest galaxies	0.55	20

REFERENCES.—(1) This paper. (2) McMillan et al. 1993. (3) Tonry 1991. (4) Bridges,Hanes, & Harris 1991. (5) Hamuy et al. 1991. (6) Geisler & Forte 1990. (7) Bothun, Caldwell, & Schombert 1989. (8) Aaronson et al. 1989. (9) Faber et al. 1989. (10) Pierce 1989. (11) Ferguson & Sandage 1988. (12) Dressler et al. 1987. (13) Caldwell & Bothun 1987. (14) Aaronson & Mould 1983. (15) Aaronson et al. 1981. (16) Aaronson, Mould, & Huchra 1980. (17) Visvanathan & Sandage 1977. (18) de Vaucouleurs, 1977. (19) Dawe & Dickens 1976. (20) de Vaucouleurs 1975.

are from this paper, while for Ursa Major the H I fluxes are from Huchtmeier & Richter (1989) and the I-band infrared luminosities from Pierce & Tully (1988). Galaxies in Fornax, a much denser cluster than the loose spiral-rich Ursa Major cluster, should be more affected by environmental effects. But Figure 5 shows that the $M_{\text{H I}}/L_I$ ratios in Fornax and Ursa Major are identical, indicating that Fornax galaxies are *not* H I deficient compared to galaxies in a low density environment. Furthermore, residuals around the Fornax Tully-Fisher fits (either from eq. [1] or eq. [3]) are not functions of the projected radius from the cluster center. This indicates that it is very unlikely that the H I layers in Fornax galaxies have been truncated up to the rising part of the rotation curve, since this effect would presumably get worse toward the center of the cluster. All these factors lead us to adopt the default assumption that the rotational properties of the galaxies and the Tully-Fisher relation derived from the H I data are normal.

7. DISCUSSION

First we compared our distance measurement with previous results. Table 3 shows values of the distance modulus of Fornax relative to Virgo as measured by various authors using methods both similar and dissimilar to the I-band Tully-Fisher relation used here. We include only research in which both clusters were studied in a single project. We did not try to infer a relative distance by comparing individual results for Fornax or Virgo published in different papers. Within the errors, our results agree with most of the recent work, except for a slight disagreement with the result of McMillan et al. (1993), who used the planetary nebulae luminosity function, a method thought to be very precise. Also, the results of Geisler & Forte (1990) and Caldwell & Bothun (1987) seem very low.

To see how our results affect the present picture of the velocity field in the Local Supercluster, we need to calculate a new value of the infall velocity of the Local Group toward Virgo. For the heliocentric velocity of Fornax and Virgo, we take the values of 1450 ± 34 km s^{-1} (Held & Mould 1994) and 1151 ± 38 km s^{-1} (Huchra 1985), which we correct in the usual way ($300 \sin l \cos b$) to the rest frame of the Local Group. For the Fornax/Virgo distance ratio, we assume the value 0.97 ± 0.07, inferred from their relative distance modulus calculated previously and identify the center of the clusters with NGC 1399 and M87, respectively. To obtain the infall velocity of the Local Group toward Virgo, we use the Virgocentric flow model described by Schechter (1980) and Aaronson et al. (1982). It assumes that the Local Supercluster is spherically symmetric with a density profile varying as $r^{-\gamma}$ (r being the distance from Virgo) and is superposed on a uniform density background. The model also depends on the peculiar velocity of the Local Group. In the linear approximation of the model (Schechter 1980, eq. [2]; Aaronson et al. 1982, eq. [B1]), using $\gamma = 2$ (Yahil, Sandage, & Tammann 1980), we obtain a value of 224 ± 90 km s^{-1} for the infall velocity of the Local Group toward Virgo. A nonlinear model gives a value some 10% higher. This result agrees well with the result of 257 ± 32 km s^{-1} from Aaronson et al. (1982), who used a large number of spirals in the Local Supercluster and the nonlinear formulation of the model.[1] It also agrees with many of the latest results by other authors (e.g., 239 ± 40 km s^{-1} by Jerjen & Tammann 1993). It should be noted that this result is independent of the zero point adopted for the distance scale; it

[1] The relevant model is solution 2 in Table 1 of Aaronson et al. (1982). Those authors preferred solution 3.1, which had additional parameters amounting to a total (pattern plus local standard of rest) infall velocity of the Local Group toward Virgo of 331 ± 41 km s^{-1}.

depends on *relative* distances only. Because the infall velocity of the Local Group is model dependent, it is harder to compare our results with those from various groups. In fact, with all the models being highly idealized, the difference between the models and reality is probably a more significant issue than the difference between the models themselves. Applying the Yahil, Tammann, & Sandage (1977) correction for the Sun's motion in the Local Group instead of that used here, we would have obtained a higher infall velocity of 306 ± 93 km s^{-1}.

To derive an absolute distance to Fornax, we need to set the zero point of the distance scale. We will look at two ways of doing this. First, we will follow the absolute calibration of the *I*-band Tully-Fisher relation done by Pierce & Tully (1988), and second, we will use the direct measurement of the distance to Virgo (M100) by Freedman et al. (1994), who used Cepheids.

First, Pierce & Tully (1988) provide an absolute calibration of the *B*-, *R*-, and *H*-band Tully-Fisher relation based on the local calibrators NGC 224, NGC 598, and NGC 2403. Unfortunately, for the *I*-band calibration, only NGC 2403 photometry could be used. Therefore, this absolute calibration cannot be precise. From Pierce & Tully, we take for NGC 2403 the parameters $M_I = -20.27$ mag, $\Delta V_{20} = 257$ km s^{-1}, and $i = 57° \pm 3°$. For the velocity width, we assume an error of 5 km s^{-1}. For the absolute magnitude, we assume an error of 0.05 mag on the measurement of the apparent magnitude, and we add errors of 0.13, 0.05, and 0.4 mag due, respectively, to the measurement errors on the distance modulus to NGC 2403 (Tammann & Sandage 1968), the measurement errors on the distance modulus to the Large Magellanic Cloud (Welch et al. 1987), and the scatter in the Tully-Fisher relation. We constrain the slope of the Tully-Fisher relation for NGC 2403 to be the one derived in § 5 for Fornax and Virgo (-8.78 ± 0.41), and we take into account the error on the zero point of the fitted relation. This way, we derive the absolute zero point of the relation to be -20.39 ± 0.46 mag, and we find a distance modulus for Fornax of 30.76 ± 0.47 mag. This in turn gives an absolute distance to Fornax of 14.2 ± 3.1 Mpc.

Second, Freedman et al. (1994) obtained a direct measurement of the distance to the Virgo galaxy M100 using Cepheids and the *Hubble Space Telescope*. They measured a true distance modulus to M100 of 31.6 ± 0.20 mag. Owing to the extended nature of the Virgo Cluster, additional uncertainties arise in the distance of Virgo. We adopt here the value quoted by Freedman et al. (1994) of 31.16 ± 0.42 mag. Combining this with the distance modulus of Fornax relative to Virgo determined in § 5 (-0.06 ± 0.15 mag), we obtain a true distance modulus to Fornax of 31.10 ± 0.45 mag. This yields an absolute distance to Fornax of 16.6 ± 3.4 Mpc. This measurement and the previous one agree within the errors.

Since both results are independent, we adopt for the distance of Fornax the mean of the two, 15.4 ± 2.3 Mpc (an absolute distance modulus of 30.94 ± 0.33 mag). This result agrees with most of the recent work done on the absolute distance of Fornax (e.g., 30.57 ± 0.20 mag by Aaronson et al. 1989; 31.44 ± 0.32 mag by Hamuy et al. 1991; 14.8 ± 0.3 Mpc by Tonry 1991) including those of McMillan et al. (1993; 31.14 ± 0.14 mag) and Geisler & Forte (1990; 31.00 ± 0.25 mag) for which a discrepancy existed regarding the distance of Fornax relative to Virgo. The result of Caldwell & Bothun (1987) still disagrees with ours.

Having obtained the infall motion of the Local Group toward Virgo, it is possible to use the calculated Fornax distance to measure the Hubble constant. Correcting the mean velocity of Fornax (relative to the Local Group) for the projection of the Local Group infall velocity in its direction, we obtain an estimate of the true velocity of Fornax. This gives 1148 ± 70 km s^{-1}, and thus we obtain a Hubble constant of $H_0 = 75 \pm 12$ km s^{-1} Mpc^{-1}. This value agrees with many of the latest measurements of the Hubble constant favoring values around 80 km s^{-1} Mpc^{-1} (e.g., 80 ± 17 km s^{-1} Mpc^{-1} by Freedman et al. 1994, and 85 ± 10 km s^{-1} Mpc^{-1} by Pierce & Tully 1988). However, it disagrees with values of H_0 lower than 60 km s^{-1} Mpc^{-1}. It should be noted that the value obtained for the Hubble constant is strongly model dependent and does not take into account any peculiar velocity of either Fornax or Virgo.

8. CONCLUSION

By improving the quantity and quality of optical and 21 cm observations of galaxies in the Fornax Cluster, we have shown that Fornax is $3\% \pm 7\%$ closer to our Galaxy than the Virgo Cluster. The redshift difference between Fornax and Virgo can be understood in the context of a flow model in which the Local Group has a large infall velocity toward Virgo compared with that of Fornax. A simple variant of the model yields a value of 224 ± 90 km s^{-1} for the Local Group infall velocity.

These results will be important in constraining H_0 because they reduce the dependence of the Hubble constant determination on detailed knowledge of the velocity field. Because Virgo and Fornax are on opposite sides of the Local Group, the motion of the observer is partially factored out of the determination. The problem can be revisualized as measuring the expansion rate of Fornax from Virgo. Distance information is still critical, however, and this is being supplied by the *HST* Key Project (Kennicutt, Freedman, & Mould 1995).

We thank the staffs of the Mount Stromlo and Siding Spring Observatories and the Parkes Observatory for their assistance and V. Ford, K. Sebo, and B. Stappers for their participation in the observations. We are grateful to M. Han for making his SFOTO package available to us and to S. Meatheringham for porting the package. M. B. acknowledges the support of an Australian DEET Overseas Postgraduate Research Scholarship and a Canadian NSERC Postgraduate Scholarship.

REFERENCES

Aaronson, M., Dawe, J. A., Dickens, R. J., Mould, J. R., & Murray, J. B. 1981, MNRAS, 195, 1P
Aaronson, M., Huchra, J., Mould, J., Schechter, P. L., & Tully, R. B. 1982, ApJ, 258, 64
Aaronson, M., & Mould, J. 1983, ApJ, 265, 1
Aaronson, M., Mould, J. R., & Huchra, J. P. 1980, ApJ, 237, 655
Aaronson, M., et al. 1989, ApJ, 338, 654
Ables, J. G., Cooper, B., Hunt, A., Moorey, G., & Brooks, J. 1975, Rev. Sci. Instrum., 46, 284
Arnaboldi, M., Freeman, K. C., Hui, X., Capaccioli, M., & Ford, H. 1994, ESO Messenger, 76, 40
Bessell, M. S. 1995, PASP, 107, 672

Bicknell, G. V. 1992, ApJ, 399, 1
Bothun, G. D., Caldwell, N., & Schombert, J. M. 1989, AJ, 98, 1542
Bothun, G. D., Schommer, R. A., & Sullivan, W. T. 1984, AJ, 89, 466
Bridges, T. J., Hanes, D. A., & Harris, W. E. 1991, AJ, 101, 469
Burstein, D., & Heiles, C. 1982, AJ, 87, 1165
Burstein, D., Rubin, V. C., Ford, K. W., Jr., & Whitmore, B. C. 1986, ApJ, 305, L11
Caldwell, N., & Bothun, G. D. 1987, AJ, 94, 1126
Cayatte, V., van Gorkom, J. H., Balkowski, C., & Kotanyi, C. 1990, AJ, 100, 604
Chincarini, G., & de Souza, R. 1985, A&A, 153, 218
Chincarini, G. L., Giovanelli, R., & Haynes, M. P. 1983, ApJ, 269, 13
Dawe, J. A., & Dickens, R. D. 1976, Nature, 263, 395
de Vaucouleurs, G. 1975, in Stars and Stellar Systems 9, ed. A. Sandage, M. Sandage, & J. Kristian (Chicago: Univ. Chicago Press), 557
———. 1977, Nature, 266, 126
Dressler, A., Lynden-Bell, D., Burstein, D., Davies, D., Faber, S., Terlevich, R., & Wegner, G. 1987, ApJ, 313, 42
Faber, S. M., Wegner, G., Burstein, D., Davies, R. L., Dressler, A., Lynden-Bell, D., & Terlevich, R. V. 1989, ApJS, 69, 763
Feigelson, E. D., & Babu, G. J. 1992, ApJ, 397, 55
Ferguson, H. C. 1989, AJ, 98, 367
Ferguson, H. C., & Sandage, A. 1988, AJ, 96, 1520
Freedman, W. L., et al. 1994, Nature, 371, 757
Freeman, K. C. 1979, in Photometry, Kinematics and Dynamics of Galaxies, ed. D. Evans (Austin: Univ. Texas Press), 85
Geisler, D., & Forte, J. C. 1990, ApJ, 350, L5
Giovanelli, R., & Haynes, M. P. 1983, AJ, 88, 881
Graham, J. A. 1982, PASP, 94, 244
Grillmair, C. J. 1992, Ph.D. thesis, Australian National Univ.
Grillmair, C. J., Freeman, K. C., Bicknell, G. V., Carter, D., Couch, W. J., Sommer-Larsen, J., & Taylor, K. 1994, ApJ, 422, L9
Guhathakurta, P., van Gorkom, J. H., Kotanyi, C. G., & Balkowski, C. 1988, AJ, 96, 851
Gunn, J. E. 1988, in ASP Conf. Ser. Vol. 4, The Extragalactic Distance Scale, ed. S. van den Bergh & C. J. Pritchet (San Francisco: ASP), 344
Hamuy, M., Phillips, M. M., Maza, J., Wischnjewsky, M., Uomoto, A., Landolt, A. U., & Khatwani, R. 1991, AJ, 102, 208
Han, M. S. 1991, Ph.D. thesis, California Institute of Technology
Held, E. V., & Mould, J. R. 1994, AJ, 107, 1307
Huchra, J. P. 1985, in ESO Workshop on the Virgo Cluster, ed. O. G. Richter & B. Bongelli (Garching: ESO), 181
Huchtmeier, W. K., & Richter, O.-G. 1989, A General Catalogue of H I Observations of Galaxies (New York: Springer-Verlag)
Jerjen, H., & Tammann, G. 1993, A&A, 276, 1
Kennicutt, R., Freedman, W., & Mould, J. 1995, AJ, 170, 1476
Landolt, A. U. 1992, AJ, 104, 340
Lauberts, A. 1982, The ESO/Uppsala Survey of the ESO (B) Atlas (Munich: European Southern Observatory)
Lauberts, A., & Valentijn, E. 1989, The Surface Photometry Catalogue of the ESO/Uppsala Galaxies (Munich: European Southern Observatory)
Mathewson, D., Ford, V., & Buchhorn, M. 1992, ApJS, 81, 413
McMillan, R., Ciardullo, R., & Jacoby, G. H. 1993, ApJ, 416, 62
Mould, J., Martin, S., Bothun, G., Huchra, J., & Schommer, B. 1995, ApJS, 96, 1
Mould, J. R., et al. 1991, ApJ, 383, 467
Phillips, M. M. 1993, ApJ, 413, L105
Pierce, M. J. 1989, ApJ, 344, L57
Pierce, M. J., & Tully, R. B. 1988, ApJ, 330, 579
Roth, J., Mould, J. R., & Staveley-Smith, L. 1994, AJ, 108, 851
Rubin, V. C., Whitmore, B. C., & Ford, W. K., Jr. 1988, ApJ, 333, 522
Schechter, P. L. 1980, AJ, 85, 801
Schröder, A., & Richter, O.-G. 1995, in prepration
Staveley-Smith, L. 1985, Ph.D. thesis, Manchester Univ.
Tammann, G. A., & Sandage, A. 1968, ApJ, 151, 825
Tonry, J. L. 1991, ApJ, 373, L1
Visvanathan, N., & Sandage, A. 1977, ApJ, 216, 214
Welch, D. L., McLaren, R. A., Madore, B. F., & McAlary, C. W. 1987, ApJ, 321, 162
Whitmore, B. C., Forbes, D. A., & Rubin, V. C. 1988, ApJ, 333, 542
Wilson, W. E., Davis, E. R., Loone, D. G., & Brown, D. R. 1992, J. Electr. Electron. Eng. Australia, 12, 187
Yahil, A., Sandage, A., & Tamman, G. 1980, in Physical Cosmology, Les Houches 1979, ed. R. Balian, J. Audouze, & D. Schramm (Amsterdam: North Holland), 127
Yahil, A., Tammann, G., & Sandage, A. 1977, ApJ, 217, 903
Zwaan, M. A., van der Hulst, J. M., de Blok, W. J. G., & McGaugh, S. S. 1995, MNRAS, 273, L35